European Journal of Pharmaceutical Sciences 160 (2021) 105756

Contents lists available at ScienceDirect

European Journal of Pharmaceutical Sciences

journal homepage: www.elsevier.com/locate/ejps

Anti-inflammatory activity of *ortho*-trifluoromethoxy-substituted 4-piperidione-containing mono-carbonyl curcumin derivatives in vitro and in vivo

Ziqing Wang, Wenwen Mu, Pengxiao Li, Guoyun Liu *, Jie Yang *

School of Pharmaceutical Sciences, Liaocheng University, 1 Hunan Street, Liaocheng, Shandong 252059, China

ARTICLE INFO

Keywords:
Mono-carbonyl curcumin derivatives
Anti-inflammatory
Raw264.7 macrophages
Colitis
Ortho-trifluoromethoxy-substituted 4-piperidione

ABSTRACT

Curcumin was reported as an anti-inflammatory agent. However, curcumin's poor bioavailability limited its clinical utility. Here, thirty *ortho*-substituted mono-carbonyl curcumin derivatives, containing acetone, cyclopentanone, cyclohexanone or 4-piperidione (*N*—H, *N*-methyl or *N*-acrylyl) moieties replacing β-diketone moiety of curcumin, were investigated for anti-inflammatory activity. Two active *ortho*-trifluoromethoxy-substituted 4-piperidione-containing derivatives **22** and **24** owned good cell uptake ability, and displayed excellent anti-inflammatory activity in both lipopolysaccharide-induced Raw264.7 macrophages and a dextran sulfate sodium (DSS)-induced mouse model of colitis. They inhibited the production of nitric oxide, reactive oxygen species, malonic dialdehyde and cyclooxygenase-2; and the expression of pro-inflammatory cytokines interleukin-1β, tumor necrosis factor-α and myeloperoxidase; the phosphorylation of mitogen-activated protein kinases; and the nucleus translocation of p65. What's more, **22** or **24** oral administered reduced the severity of clinical symptoms of ulcerative colitis (body weight and disease activity index), and reduced obviously DSS-induced colonic pathological damage (the colon length and histopathology analysis). These results suggested that *ortho*-trifluoromethoxy-substituted 4-piperidione-containing mono-carbonyl curcumin derivatives **22** and **24** were potential anti-inflammatory agents; and offered the important information for design and discovery of more potent anti-inflammatory drug candidates.

1. Introduction

Inflammatory bowel disease (IBD), containing Crohn's disease (CD) and ulcerative colitis (UC), is a kind of chronic non-specific intestinal inflammatory disease with unclear etiology. Currently, the treatment options for patients with IBD include corticosteroids, sulfasalazine, mesalamine, and immunosuppressors or surgical treatments. However, due to a marked immune response suppression, conventional treatments have numerous side effects, and negative impacts on the quality of life of sufferers (Bryant et al., 2015; Harbord et al., 2017; Kawalec and Malinowski, 2015). Therefore, effective and safe therapeutic agents are still necessary for prevention and treatment of IBD.

Curcumin, a natural yellow pigment isolated from the rhizomes of Curcuma longa, could be applied in food coloration, cosmetics utility, and fabric dying and so on. In addition, curcumin has been shown multiple pharmacological activities, including antioxidant, anti-cancer, anti-inflammatory, antimicrobial, and cardiovascular protective effects (Chen et al., 2020). Curcumin displayed anti-inflammatory effect via inhibition of different signaling pathways such as nuclear factor kappa-B (NF-κB), toll-like receptor 4 (TLR4) and mitogen-activated protein kinase pathways (MAPKs), and suppression of the expression of cyclooxygenase-2 (COX-2), nitric oxide (NO) and pro-inflammatory cytokines (interleukin (IL)−1β, IL-6, IL-18 and tumor necrosis factor-alpha (TNF-α)) (Karimian et al., 2017; Zhou et al., 2015). However curcumin's poor bioavailability, unstability and rapid degradation under physiological conditions limited its clinical utility (Begum et al., 2008; Siviero et al., 2015).

Natural products are the inspiration of drug discovery, and structural modification of natural products is an important strategy in pharmaceutical discovery. The β-diketone moiety of curcumin has been considered to be responsible for its unstability, rapid degradation and poor bioavailability (Singh et al., 2019; Wiggers et al., 2017). In recent years, a lot of mono-carbonyl curcumin derivatives were developed with improved biological activities in preventing and treating various diseases (Dinkova-Kostova et al., 2007; He et al., 2018) (such as cancer, inflammation, et al.), through regulating a variety of molecular targets in cells, such as inhibiting NF-κB pathways, activating c-Jun N-terminal kinase (JNK) pathway or inhibiting B-cell lymphoma 2 (Bcl-2)

* Corresponding author.
E-mail addresses: guoyunliu@126.com (G. Liu), yangjie1110@163.com (J. Yang).

https://doi.org/10.1016/j.ejps.2021.105756
Received 20 November 2020; Received in revised form 5 February 2021; Accepted 9 February 2021
Available online 12 February 2021

expression, etc. (Chen et al., 2018; Zhu et al., 2016). The structure designs of mono-carbonyl curcumin derivatives not only replace β-diketone by acythesizedetone, but also combine with cyclopentanone, cyclohexanone, 4-piperidone, or *N*-substituted-4-piperidone moieties and so on (Dai et al., 2015; Li et al., 2019; Liu et al., 2016; Wu et al., 2013; Yang et al., 2020). In addition, among the design strategies of mono-carbonyl curcumin derivatives, "*ortho* effect", that *ortho*-substituents on the phenyl ring can contribute to the improvement of biological activity, is emphasized and utilized. For example, the presence of a ortho group was proven to strengthen significantly the cytotoxicity of mono-carbonyl curcumin derivatives (Dai et al., 2015; Liu et al., 2016), cinnamaldehyde derivatives (Chew et al., 2010) and chalcone derivatives (Gan et al., 2013), the potency of curcumin derivatives in inducing phase II enzymes (Dinkova-Kostova et al., 2001), and the interaction with certain target proteins by a conformational change of a ligand (Schönherr and Cernak, 2013). Besides, the introduction of fluorine and fluorinated groups into potential drug candidates is a commonly employed approach to improve their biological activities, including metabolic stability, high lipophilicity, enhanced binding interactions, and bioavailability (Hagmann, 2008; Yerien et al., 2016).

Therefore, in this study, we designed and chose thirty mono-carbonyl curcumin derivatives with drawing/donoring groups (hydroxyl, methoxy, fluoro, trifluoromethyl and trifluoromethoxy) attaching to *ortho*-position on the aromatic ring, together with acetone, cyclopentanone, cyclohexanone, 4-piperidione (*N*—H, *N*-methyl, and *N*-acrylyl) moieties respectively. Then, we focused on their anti-inflammatory effect in lipopolysaccharide (LPS)-stimulated Raw264.7 macrophages and a dextran sulfate sodium (DSS)-stimulated mouse model of colitis, for the sake of seeking the potent anti-inflammatory agents in vivo.

2. Result and discussion

2.1. Mono-carbonyl curcumin derivatives

Thirty mono-carbonyl curcumin derivatives with drawing/donoring groups (hydroxyl, methoxy, fluoro, trifluoromethyl and trifluoromethoxy) in the *ortho* position were designed and synthesized by our laboratories (Liu et al., 2018; Liu et al., 2018; Yang et al., 2018; Yang et al., 2018; Zhang et al., 2018). β-diketone moiety of curcumin were replaced with acetone, cyclopentanone, cyclohexanone, and 4-piperidione (*N*—H, *N*-methyl, and *N*-acrylyl) moieties respectively.

2.2. In vitro study

2.2.1. The inhibitory effect of derivatives on the LPS-induced no production

The macrophage plays a critical role in the inflammation as a response to injury or infection (Chawla et al., 2011). LPS is widely used as the inducer of inflammation of macrophages, and it could induce the production of NO, ROS, cytokines and so on. LPS-induced Raw264.7 macrophage cells is a classical model to cause NO production. NO is a key inflammatory intermediate (Nagy et al., 2007). Excessive NO production can cause significant inflammatory damage or disease. Inhibitors of NO production might be potential anti-inflammatory agents.

Firstly, a series of mono-carbonyl curcumin derivatives were tested for their inhibitory effect on the NO production in the LPS-induced Raw264.7 macrophage cells. Results were expressed as IC_{50} (Table 1), the half maximal inhibitory concentration. From an "β-diketone moiety modification" perspective, cyclopentanone and cyclohexanone modifications showed little or no contribution to improve the anti-inflammation activity. For acetone derivatives, 2-hydroxy-substituted derivative **1**, showed the best activity (2.47 μM); for 4-piperidione derivatives, 2-methoxy- and 2-trifluoromethoxy-substituted derivatives **10** and **22**, showed excellent activity (2.48 and 2.73 μM); for *N*-methyl-4-piperidone derivatives, 2-methoxy-substituted derivatives **11**, showed good activity (3.66 μM); for *N*-acrylyl-4-piperidone derivatives, 2-methoxy- and 2-trifluoromethoxy-derivatives **12** and **24**, showed excellent activity (2.77 and 2.02 μM) (Fig. 1).

Unfortunately, there were no obvious the structure-activity relationship. However, over half derivatives were more potent than their parent molecule curcumin (19.43 μM). Moreover, the IC_{50} values of eight derivatives (**1, 4, 10, 11, 12, 18, 22**, and **24**) were less than 5 μmol/L, and all of eight active derivatives exhibited low cytotoxicity. (Fig. 2)

2.2.2. Effects of active derivatives on the protective properties against t-BHP-induced cytotoxicity in the Raw264.7 macrophage cells

Oxidative stress plays a key role in the inflammation, and is related to IBD (Dudzińska et al., 2018). Oxidative stress could cause the overproduction of ROS, and further aggravate the inflammatory reaction (Lei et al., 2015). In order to supplement to the results of initial screening, we further chose these eight active derivatives to test the effects on the protective properties against *tert*-butyl hydroperoxide (*t*-BHP)-induced cytotoxicity in Raw264.7 macrophage cells, an oxidative stress model, using an MTT assay. As shown in Fig. 3, after treatment with *t*-BHP, cell viability was decreased in a concentration-dependent manner relative to the control group. All of eight active derivatives protected remarkably the cells from *t*-BHP-induced oxidative cytotoxicity along with 2 mM *t*-BHP. Moreover, when treatment with 2.5 μM active derivatives, the cell viability was increased to above 70%. However, the same concentration of curcumin didn't show any protective effect, and treatment with 20 μM curcumin could increase the cell viability to about 70%. These results suggested that these eight derivatives owned more protective properties against *t*-BHP-induced oxidative cytotoxicity than curcumin in the Raw264.7 macrophage cells. In addition, **1, 10, 22** and **24** were more effective than **4, 11, 12** and **18** by comparing the effect of 0.5 μM.

2.2.4. Effect of cellular uptake activity

Next, these active derivatives **1, 10, 22** and **24** were examined to compare their cellular uptake ability according to the previously published paper (Dai et al., 2015; Kunwar et al., 2008) with some modifications (Liu et al., 2021). Fig. 4A showed a comparison of four active derivatives in the cellular uptake in Raw264.7 cells by high performance liquid chromatography analysis of methanol extracted cell lysates, after treatment with 50 μM derivatives for different time. As shown in Fig. 4A, **22**, and **24** displayed good cellular uptake in cells, compared with **1** and **10**. Notably, **22**, and **24** contained trifluoromethoxy groups; **1 and 10**

Table 1
The inhibitory effect of derivatives on the NO production.

	Num	IC_{50}(μM)	Num	IC_{50}(μM)	Num	IC_{50}(μM)	Num	IC_{50}(μM)	Num	IC_{50}(μM)
	2-OH		2–OCH_3		2-CF_3		2-OCF_3		2-F	
acetone	**1**	2.47 ± 0.02	**7**	10.42 ± 0.96	**13**	19.79 ± 1.32	**19**	>200	**25**	18.06 ± 0.96
cyclopentanone	**2**	24.46 ± 0.44	**8**	>100	**14**	49.95 ± 2.75	**20**	52.01 ± 4.72	**26**	>100
cyclohexanone	**3**	9.89 ± 0.76	**9**	13.51 ± 1.57	**15**	72.81 ± 6.30	**21**	18.98 ± 1.13	**27**	27.26 ± 1.37
4-piperidione	**4**	3.70 ± 0.35	**10**	2.48 ± 0.57	**16**	25.27 ± 1.33	**22**	2.73 ± 0.54	**28**	15.72 ± 0.77
N-methyl-4-piperidione	**5**	5.22 ± 0.83	**11**	3.66 ± 0.14	**17**	8.36 ± 0.67	**23**	19.26 ± 1.48	**29**	6.07 ± 0.79
N-acrylyl-4-piperidione	**6**	17.50 ± 0.53	**12**	2.77 ± 0.70	**18**	4.89 ± 0.45	**24**	2.02 ± 0.08	**30**	5.80 ± 0.34
	Cur	19.43 ± 1.39								

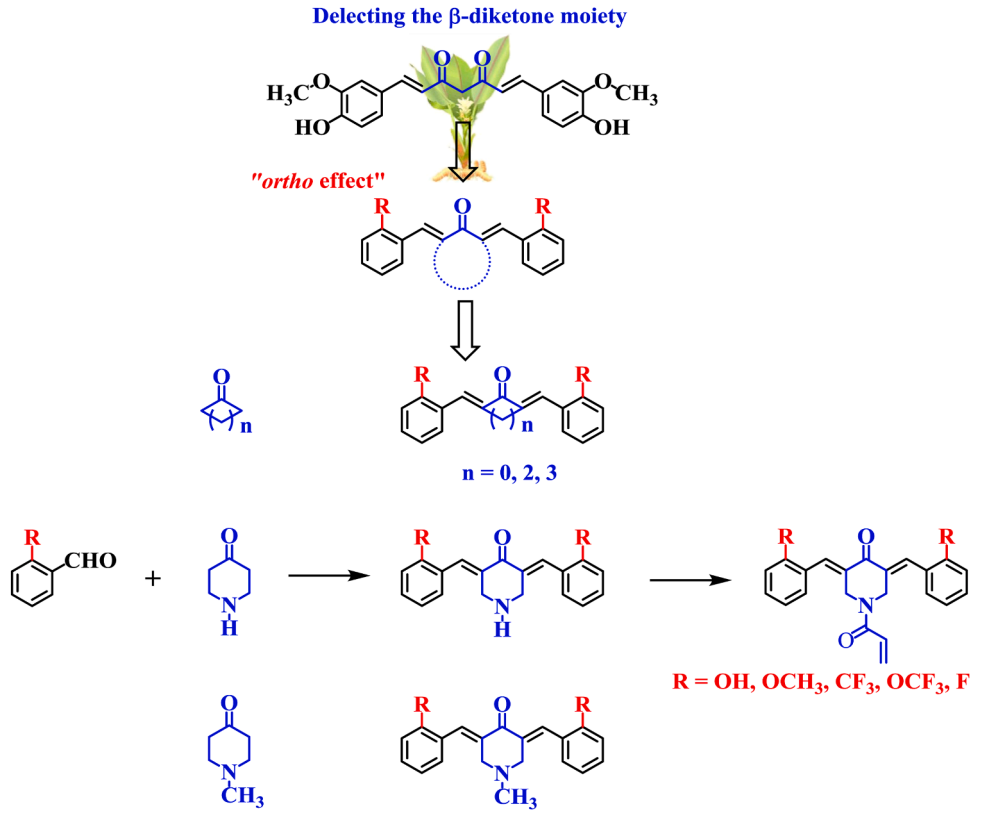

Fig. 1. Design and synthesis of mono-carbonyl curcumin derivatives.

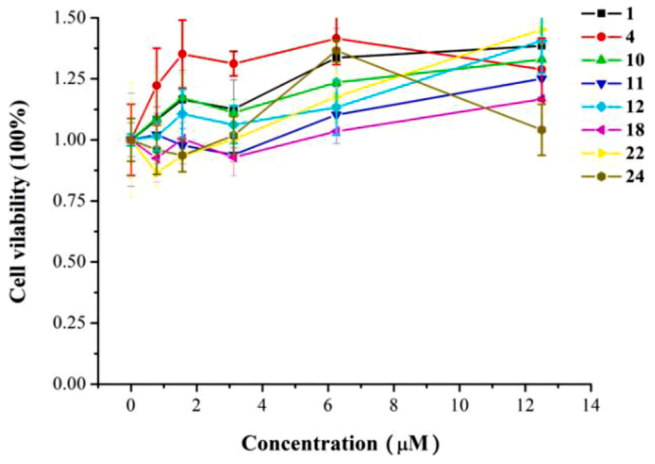

Fig. 2. Effect of eight active derivatives on cell viability in the Raw264.7 macrophage cells. Data were expressed as means ± SD (n = 3) from independent experiments.

contained hydroxyl or methoxy groups. These results provided evidences that the incorporation of fluorine-containing moieties into derivatives significantly contributed to the increased cellular uptake. Besides, it was observed that only 5.81% or 3.01% accumulated in the membrane for **22** or **24** (Fig 4B), respectively, which reflected that **22** and **24** could effectively penetrate the cellular membrane to enter the cells.

According to the initial screening in the LPS-induced NO overexpression cell model, the *t*-BHP-induced oxidative stress cell model, and cell uptake ability, we then selected two *ortho*-trifluoromethoxy-substituted derivatives **22** and **24** for the follow-up studies. The different of structures between **22** and **24** was the easily hydrolyzed amide bond of 4-piperidione. The *ortho*-trifluoromethoxy group could contribute to its improved anti-inflammatory activity, cell uptake ability and metabolic stability. Moreover, trifluoromethoxy group adopted an orthogonal direction relative to the aromatic plane, which might be contributed to the protein-ligand interactions (Müller et al., 2007).

2.2.5. *Effect on the intracellular ROS generation*

The excessive ROS production was related to the activation and aggravation of the inflammation (Mittal et al., 2014). To investigated the anti-inflammatory mechanism of **22** and **24**, we tested the effect of **22** and **24** on the production of ROS in LPS-induced Raw264.7 macrophage cells. As shown in Fig. 5, the ROS levels in the LPS-induced cells substantially increased compared to the control cells. When treatment with **22** or **24** at the same time, intracellular ROS levels were significantly decreased in a concentration-dependent manner relative to treatment with LPS only. And, **22** showed little more activity than **24**. It was suggested that **22** and **24** maybe play anti-inflammatory role via inhibiting the production of ROS.

2.2.6. *Evaluation of ability of **22** and **24** to inhibit LPS-mediated IL-1β and TNF-α production*

Pro-inflammatory cytokines, secreted by immune cells, has been reported to serve vital roles in host defense (Akira et al., 2006). Herein, we selected IL-1β and TNF-α as the representatives to evaluated the inhibitory effects of **22** and **24** on pro-inflammatory cytokines in the LPS-induced Raw264.7 macrophage cells, and the expressions were detected by ELISA. As shown in Fig. 6, the formations of IL-1β and TNF-α in the control cells were low, but they were significantly increased when treatment with LPS only. When treatment with **22** or **24** at the same time, the expressions of IL-1β and TNF-α was inhibited in a concentration-dependent manner relative to the LPS cells. And, **22** showed little more activity than **24**. So, this result further indicated that **22** and **24** were the inspiring anti-inflammatory compounds owning the ability to inhibit LPS-stimulated cytokine expressions.

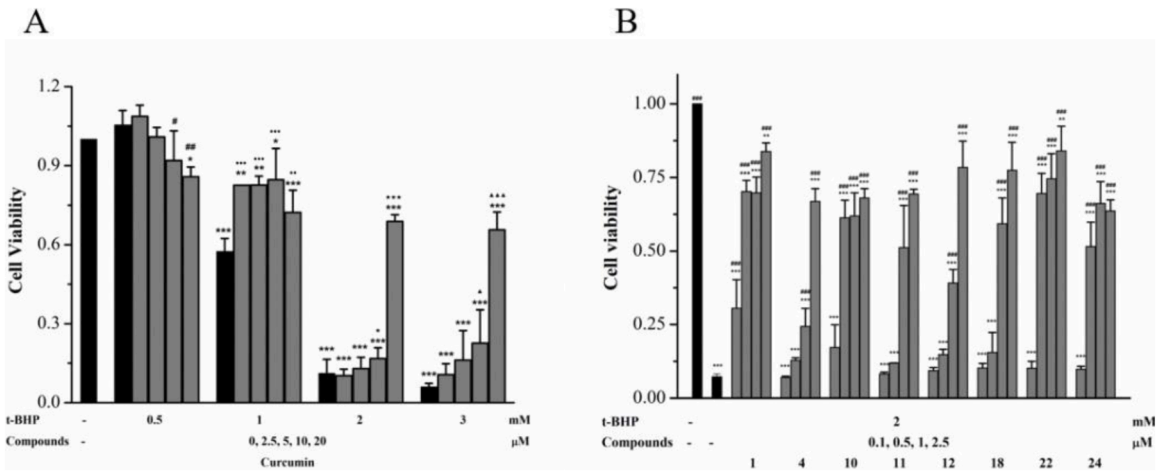

Fig. 3. Effects of eight active derivatives on the *t*-BHP-induced RAW264.7 macrophage cell cytotoxicity. (A) RAW 264.7 macrophage cells were subjected to curcumin for 24 h, subsequently induced with different concentrations of *t*-BHP for 3 h. $^{*}p < 0.05$, $^{**}p < 0.01$, $^{***}p < 0.001$, compared with the control group. $^{\#}p < 0.05$, $^{\#\#}p < 0.01$, $^{\#\#\#}p < 0.001$, compared with the 0.5 mM *t*-BHP group. $^{\bullet}p < 0.05$, $^{\bullet\bullet}p < 0.01$, $^{\bullet\bullet\bullet}p < 0.001$, compared with the 1 mM *t*-BHP group. $^{\star}p < 0.05$, $^{\star\star}p < 0.01$, $^{\star\star\star}p < 0.001$, compared with the 2 mM *t*-BHP group. $^{\blacktriangle}p < 0.05$, $^{\blacktriangle\blacktriangle}p < 0.01$, $^{\blacktriangle\blacktriangle\blacktriangle}p < 0.001$, compared with the 3 mM t-BHP group. (B) RAW 264.7 macrophage cells were subjected to derivatives for 24 h, subsequently induced with *t*-BHP (2 mM) for 3 h. $^{*}p < 0.05$, $^{**}p < 0.01$, $^{***}p < 0.001$, compared with the control group. $^{\#}p < 0.05$, $^{\#\#}p < 0.01$, $^{\#\#\#}p < 0.001$, compared with the 2 mM *t*-BHP group. Measurement of cytotoxicity using the MTT assay. Data were expressed as means ± SD ($n = 3$) from independent experiments.

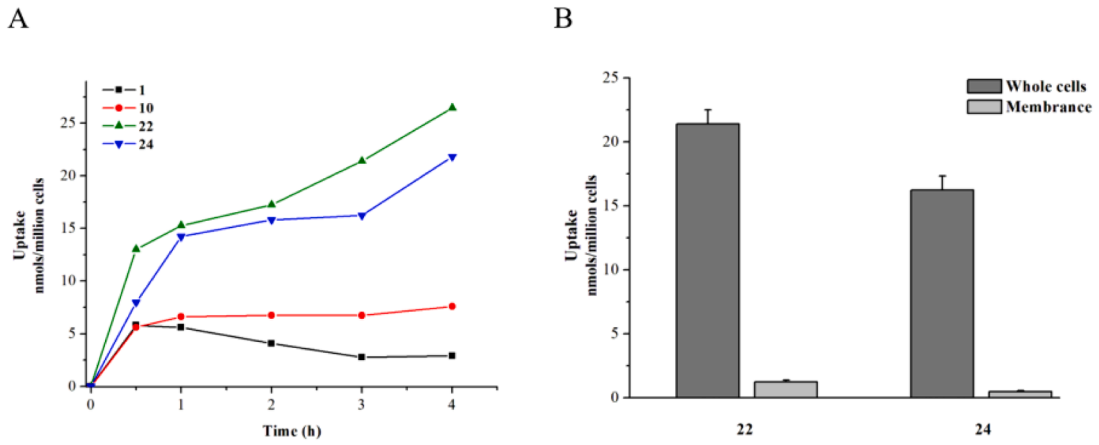

Fig. 4. Cellular uptake of four active derivatives in whole cells (A) and membrane (B).

*2.2.7. Evaluation of the ability of **22** and **24** to suppress LPS-induced COX-2 production*

COX-2 is an important regulator of inflammatory mediator production in response to LPS or other stimuli. And the upregulation of COX-2 can promote chronic inflammation. Therefore, we next evaluated the ability of **22** and **24** to modulate LPS-induced the expression of COX-2, and the levels were analyzed using western blot. As shown in Fig. 7, LPS caused a significant increase in the protein levels of COX-2 compared with the control cells. Treatment with **22** or **24** reduced the LPS-induced COX-2 expression.

These results presented above suggested that **22** and **24** could prevent LPS-induced expression of inflammatory mediators (NO, ROS, IL-1β, TNF-α and COX-2), and they were worthy of further study.

*2.2.8. Assessment of the ability of **22** and **24** to inhibit the phosphorylation of MAPKs in the LPS-induced Raw264.7 macrophage cells*

The MAPK signaling pathway is important in the expression of inflammatory factors. During the inflammatory response, the phosphorylation of MAPK proteins (p38, JNK, and ERK) is key for the activation of activating protein 1 (AP-1) and NF-κB, and the release of NO, IL-1β, TNF-α and so on in the LPS-induced macrophages. The phosphorylation levels of MAPK proteins were analyzed using western blot. As shown in Fig. 8, LPS caused the increase of the phosphorylation of p38, JNK, and ERK. Treatment with **22** could obviously decreased the phosphorylation of MAPK proteins. But, **24** showed less effect on the decrease of the phosphorylation of p-38 and p-JNK than **22**, and showed little effect on the decrease of the phosphorylation of p-ERK. This suggested that **22** and 24 could exert an anti-inflammatory activity, which was related to the prevention the activation of the LPS-induced MAPK signal pathway.

*2.2.9. Assessment of the ability of **22** and **24** to inhibit LPS-induced NF-κB activation*

NF-κB is an key transcription factor, which regulates the pro-inflammatory mediators in activated macrophages. Before macrophage cells are induced with LPS, NF-κB is inactive, is bounded with the inhibitor kappa B (IκB) and retained in the cytoplasm. When macrophage cells are stimulated, activated IκB is phosphorylated, releasing the NF-κB heterodimers (p65/p50), which then translocate into the nucleus, and further to bind to pro-inflammatory genes (Kim et al., 2016). So, the p65 nuclear translocation is an important marker for the inflammatory reaction.

To investigate if the activation of NF-κB was inhibited by **22** or **24** in

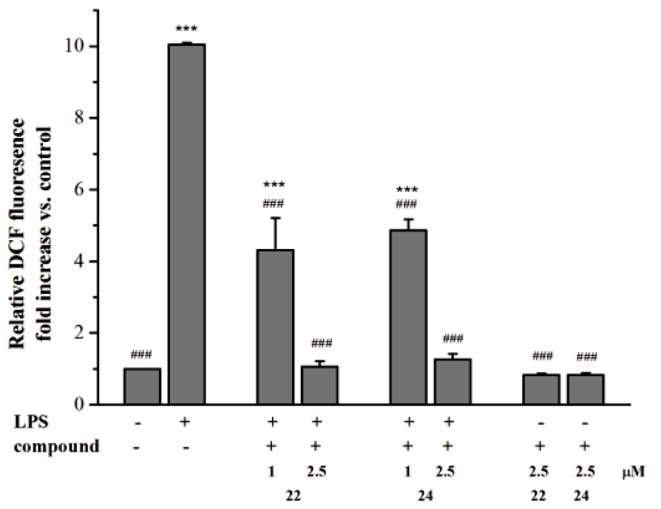

Fig. 5. Effects of the active derivatives on ROS production in the LPS-induced Raw264.7 macrophage cells, using DCFH-DA staining and flow cytometric analysis. The levels of ROS were expressed as fold change relative to the levels in the control cells. Data were expressed as means ± SD ($n = 3$) from independent experiments. $^{*}p < 0.05$, $^{**}p < 0.01$, $^{***}p < 0.001$, compared with the control group. $^{\#}p < 0.05$, $^{\#\#}p < 0.01$, $^{\#\#\#}p < 0.001$, compared with the LPS group.

the LPS-induced Raw264.7 macrophage cells, the expressions of p65 in nuclear and cytoplasmic extracts were analyzed using western blot. As shown in Fig. 9, when treatment with LPS only, the expression of p65 in the nuclei markedly increased. However, the nuclear levels of p65 were reduced obviously by **22** or **24** treatment. Meanwhile, the cytoplasmic levels of p65 were similar. Therefore, the LPS-induced increase of p65 nuclear translocation in Raw264.7 macrophage cells was suppressed obviously in **22** or **24** treatment group accoring to the relative protein expression (the nuclear levels of p65/the cytoplasmic levels of p65); that was to say, **22** and **24** could inhibit LPS-induced NF-κB activation. And, **22** showed little more activity than **24**.

2.3. *In vivo study*

A DSS-induced mouse model of colitis was used to verify whether **22** and **24** showed effective anti-inflammatory effect in vivo. UC is one of the common nonspecific IBD, which causes inflammation and ulcers in the colonic mucosa (Cosnes et al., 2011). A DSS-induced mouse model of colitis can emulate the disease characteristics of human UC, including weight loss, diarrhea, rectal bleeding, intestinal mucosal damage, and pro-inflammatory cytokine elevation. This classic model has been widely used to screen potential therapeutic agents of UC.

2.3.1. *Effect of **22** and **24** on the development of DSS-induced colitis in mice*

As shown in Fig. 10A and 10B, after 4 days of DSS treatment, the ratio of body weight change was markedly decreased in the DSS-treated group relative to the control group. The loss of body weight was remarkly reduced in 200 mg/kg/day **22**-treated group and 100 mg/kg/day **24**-treated group, in which the effects were significantly better than the effect of treatment with 300 mg/kg/day sulfasalazine (SASP), which was effective for treating UC (Singh et al., 2009), and was used as the reference anti-inflammatory drug.

The scores of disease activity index (DAI) of mice was determined according to the scoring system (Table 2) (Cooper et al., 1993; Mu et al., 2016). As shown in Fig. 10C and 10D, the scores of DAI of mice in 200 mg/kg/day **22**- or 100 mg/kg/day **24**-treated group were remarkly lower than that in the DSS- or 300 mg/kg/day SASP-treated group. The results of DAI indicated clearly that oral administration of **22** and **24** effectively alleviated the severity of clinical symptoms of colitis in the DSS-induced mouse model.

2.3.2. *Effect of **22** and **24** on the colon in the DSS-induced mouse model of colitis*

DSS administration leads to ulceration, hyperemia and bowel wall thickening, and then cause significantly decreasing of colon length, which is an obvious symptom. As shown in Fig. 11A, the colon length in the DSS group was obviously short relative to the control group. However, shortening of colon length was attenuated significantly with **22** and **24** treatments at 200 and 100 mg/kg/day respectively.

Additionally, histopathological analysis was used to test the protective effect of **22** and **24** on colitis using hematoxylin-eosin (H&E) staining, and representative images of colons and the histological scores were shown in Fig. 11B. The histological scoring system was shown in Table 3 (Mu et al., 2016). Compared with the control group, histological observation of the DSS-treated group showed a significant acute inflammatory response, which was characterized by severe lesions in the mucosa, loss of crypts, increase in neutrophil population and so on (Mazzucchelli et al., 1994). However, after treatment with **22** or **24**, the above symptoms of mice were significantly reduced in a

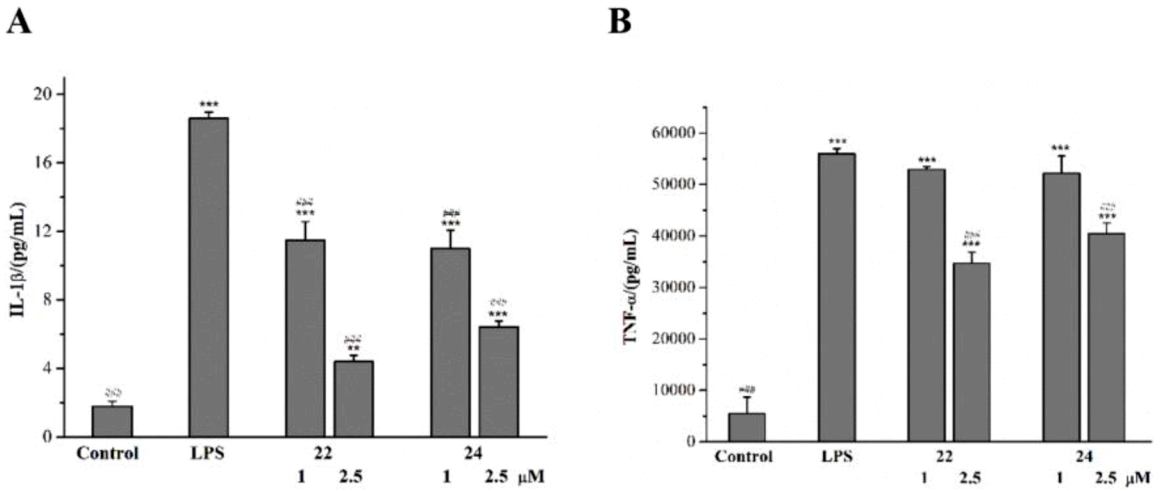

Fig. 6. Effects of the active derivatives on the expression of IL-1β and TNF-α in the LPS-induced Raw264.7 macrophage cells. Data were expressed as means ± SD ($n = 3$) from independent experiments. $^{*}p < 0.05$, $^{**}p < 0.01$, $^{***}p < 0.001$, compared with the control group. $^{\#}p < 0.05$, $^{\#\#}p < 0.01$, $^{\#\#\#}p < 0.001$, compared with the LPS group.

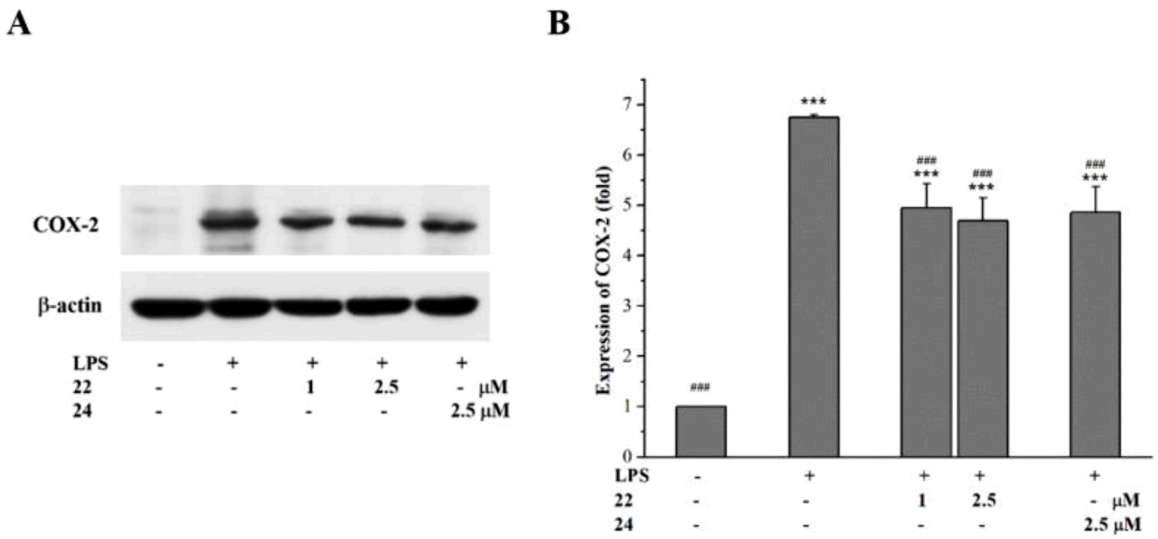

Fig. 7. **22** and **24** inhibited LPS-induced expression of COX-2 in the RAW264.7 macrophage cells. The representative images were shown here. Data were expressed as means ± SD ($n = 3$) from independent experiments. $^{*}p < 0.05$, $^{**}p < 0.01$, $^{***}p < 0.001$, compared with the control group. $^{\#}p < 0.05$, $^{\#\#}p < 0.01$, $^{\#\#\#}p < 0.001$, compared with the LPS group.

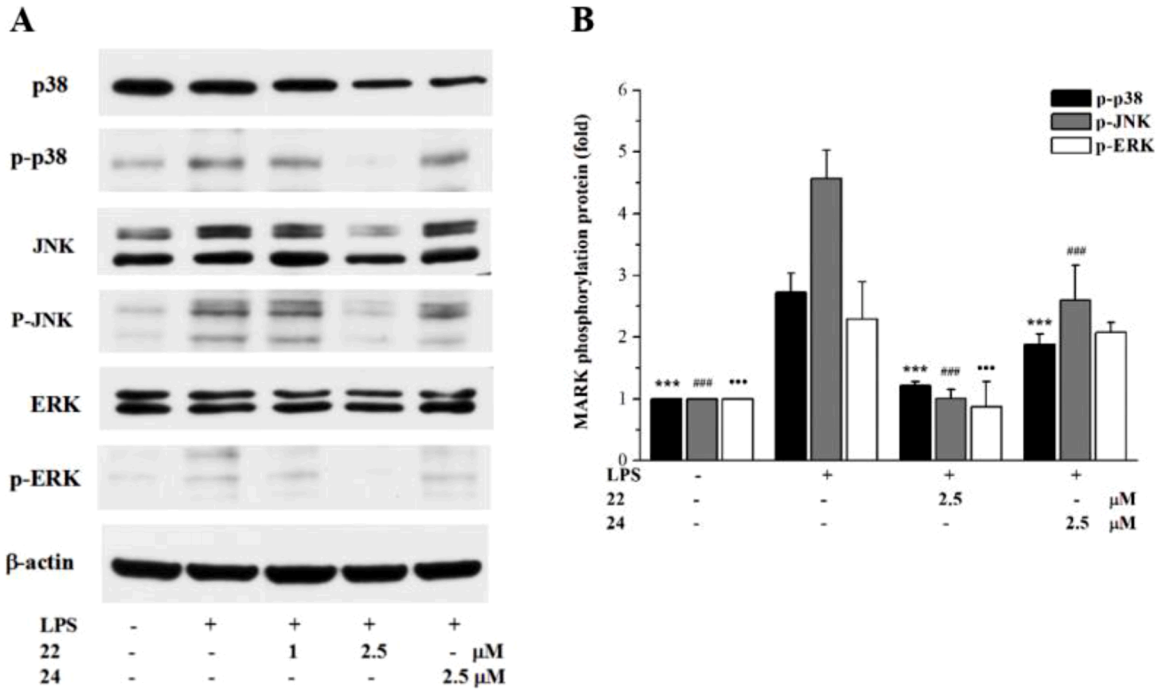

Fig. 8. Effect of **22** and **24** on the activation of MAPK signaling pathways. The representative images were shown here. Data were expressed as means ± SD ($n = 3$) from independent experiments. $^{*}p < 0.05$, $^{**}p < 0.01$, $^{***}p < 0.001$, compared with the LPS group of p-p38. $^{\#}p < 0.05$, $^{\#\#}p < 0.01$, $^{\#\#\#}p < 0.001$, compared with the LPS group of p-JNK. $^{\bullet}p < 0.05$, $^{\bullet\bullet}p < 0.01$, $^{\bullet\bullet\bullet}p < 0.001$, compared with the LPS group of p-ERK.

concentration-dependent manner relative to the DSS group. Contrasted with control group, 300 mg/kg/day SASP, 50 mg/kg/day **22**, and 50 mg/kg/day **24** groups, were reduced partially colonic tissue damage; whereas, 100 mg/kg/day **22**, and 100 mg/kg/day **24** groups, were reduced significantly colonic tissue damage. These results suggested that 100 mg/kg/day **22** or 100 mg/kg/day **24** could protect remarkably the colonic tissue against the DSS-induced damage.

*2.3.3. Evaluation of ability of **22** and **24** to inhibit DSS-mediated IL-1β and TNF-α production in colon*

In addition to histopathological analysis, we further investigated the inflammatory cytokines in the colon, and chose IL-1β and TNF-α to test the inhibitory effects of **22** and **24** on pro-inflammatory cytokines in colon tissues of DSS-induced mouse model of colitis. As shown in Fig. 12, compared with the control group, the levels of IL-1β and TNF-α increased remarkably in the DSS-treated group. After treatment with 300 mg/kg/day SASP, or different concentration of **22** and **24**, these levels were significantly inhibited, but without in a concentration-dependent manner. These results indicated that **22** and **24** could possess potent anti-inflammatory activity through inhibiting the expression of pro-inflammatory cytokines in the DSS-induced mice.

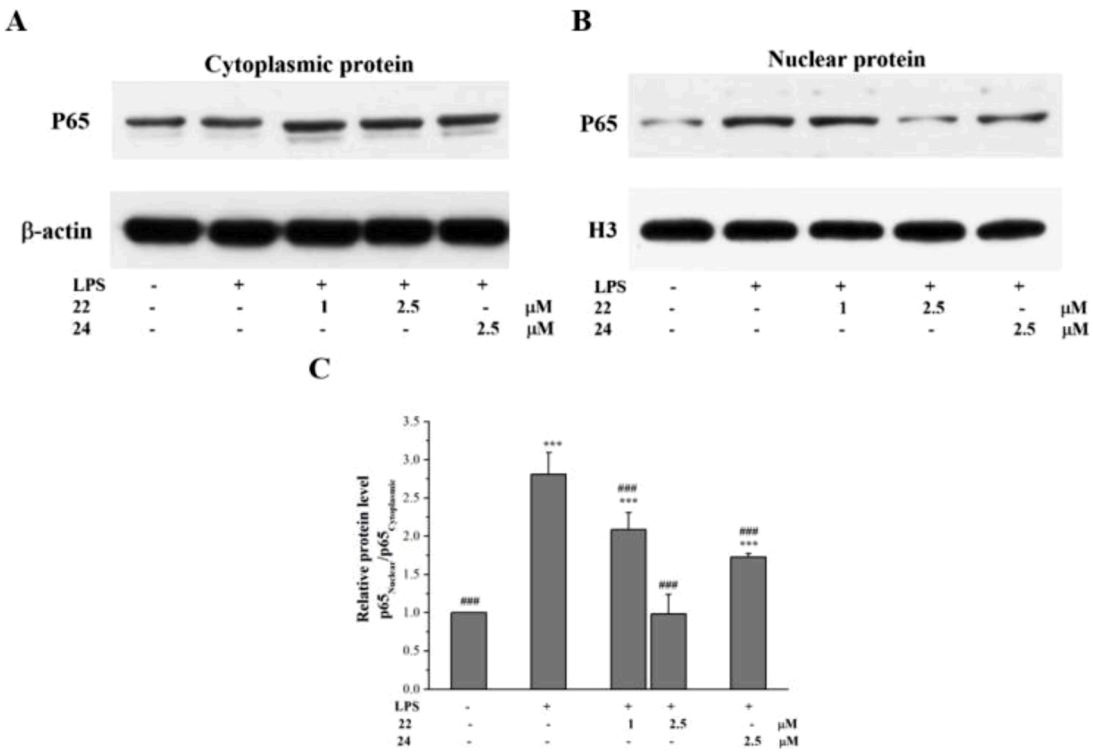

Fig. 9. Effect of **22** or **24** on the NF-κB p65 nuclear translocation. (A, B) The expression of P65 proteins of cytoplasmic and nuclear proteins were assessed by western blot analysis. The representative images were shown here. (C) Relative protein levels of nuclear and cytoplasmic P65 protein. Data were expressed as means ± SD ($n = 3$) from independent experiments. $^{*}p < 0.05$, $^{**}p < 0.01$, $^{***}p < 0.001$, compared with the control group. $^{\#}p < 0.05$, $^{\#\#}p < 0.01$, $^{\#\#\#}p < 0.001$, compared with the LPS group.

*2.3.4. Evaluation of ability of **22** and **24** to inhibit DSS-mediated NO, MDA, and MPO production in colon*

Oxidative and nitrosative stress, that the continuously excessive ROS/RNS production due to an imbalance of cellular redox homeostasis, both act as a significant role in the process of inflammation and inflammation-associated diseases (Yu et al., 2015). Here, we chose several typical indexes of oxidative and nitrosative stress to further measure. NO is a key inflammatory intermediate. Malonic dialdehyde (MDA) is an important end product of lipid peroxidation. Myeloperoxidase (MPO) is an enzyme of peroxidases found in azurophilic granules of neutrophils.

As shown in Fig. 13, the levels of NO, MDA, and MPO in the DSS-treated group significantly increased relative to the control group. When treatment with 300 mg/kg/day SASP, these levels significantly decreased compared with DSS group. These levels in 100 or 200 mg/kg/day **22** or **24** groups were lower than these levels in both DSS and 300 mg/kg/day SASP groups. These results indicated that administration of 100 or 200 mg/kg/day **22** or **24** groups could inhibit the production of RNS and ROS, and exert their anti-nitrosative and anti-oxidative stress effects, which were related to the anti-inflammatory effect. And, the inhibitory activity of the production of RNS and ROS was consistent with the inhibition of pro-inflammatory cytokines, and the reduction of the severity of clinical symptoms and the pathological damage of ulcerative colitis in the DSS-induced mice. Moreover, the anti-inflammatory effect of **22** and **24** was consistent in the DSS-induced mouse model of colitis and in the LPS-induced Raw264.7 macrophage cells.

3. Conclusion

In this paper, thirty *ortho*-substituted mono-carbonyl curcumin derivatives were designed and chose, containing acetone, cyclopentanone, cyclohexanone, or 4-piperidione (*N*—H, *N*-methyl or *N*-acrylyl) moieties replacing β-diketone moiety of curcumin. Through the initial screening, two active *ortho*-trifluoromethoxy-substituted 4-piperidione-containing mono-carbonyl curcumin derivatives **22** and **24**, owning the good cell uptake ability, inhibiting effectively the LPS-induced overexpression of NO, and protecting remarkably the Raw264.7 macrophage cells from *t*-BHP-induced oxidative cytotoxicity, were gained and chose to further study. In the LPS-induced Raw264.7 macrophage cells model, **22** and **24** showed excellent anti-inflammatory effect, which inhibited effectively the levels of ROS, the expression of pro-inflammatory cytokines (IL-1β and TNF-α), the production of COX-2, the phosphorylation of MAPKs, and the nucleus translocation of p65.

What's more, **22** and **24** exerted excellent anti-inflammatory effect in the DSS-induced mouse model of colitis. Oral administration of **22** or **24**, could reduce effectively the severity of clinical symptoms of UC (body weight change and the scores of DAI), and reduced effectively colonic tissue damage (the colon length and histopathology analysis). Furthermore, **22** and **24** displayed anti-inflammatory activity through suppressing the expression of pro-inflammatory cytokine (IL-1β and TNF-α), and the production of RNS/ROS (NO, MDA, and MPO) of colon in the DSS-induced mouse model of colitis.

This study has provided the scientific evidences that *ortho*-trifluoromethoxy-substituted 4-piperidione-containing mono-carbonyl curcumin derivatives **22** and **24** were potential anti-inflammatory agents; and offered the important information for design and discovery of more potent anti-inflammatory drug candidates. Further study will focus on the further molecular mechanism of anti-inflammatory activity, metabolism, bioavailability and toxicological effects in the animal model.

4. Materials and methods

4.1. Chemistry

All reagents and chemicals were commercially available from Sigma-

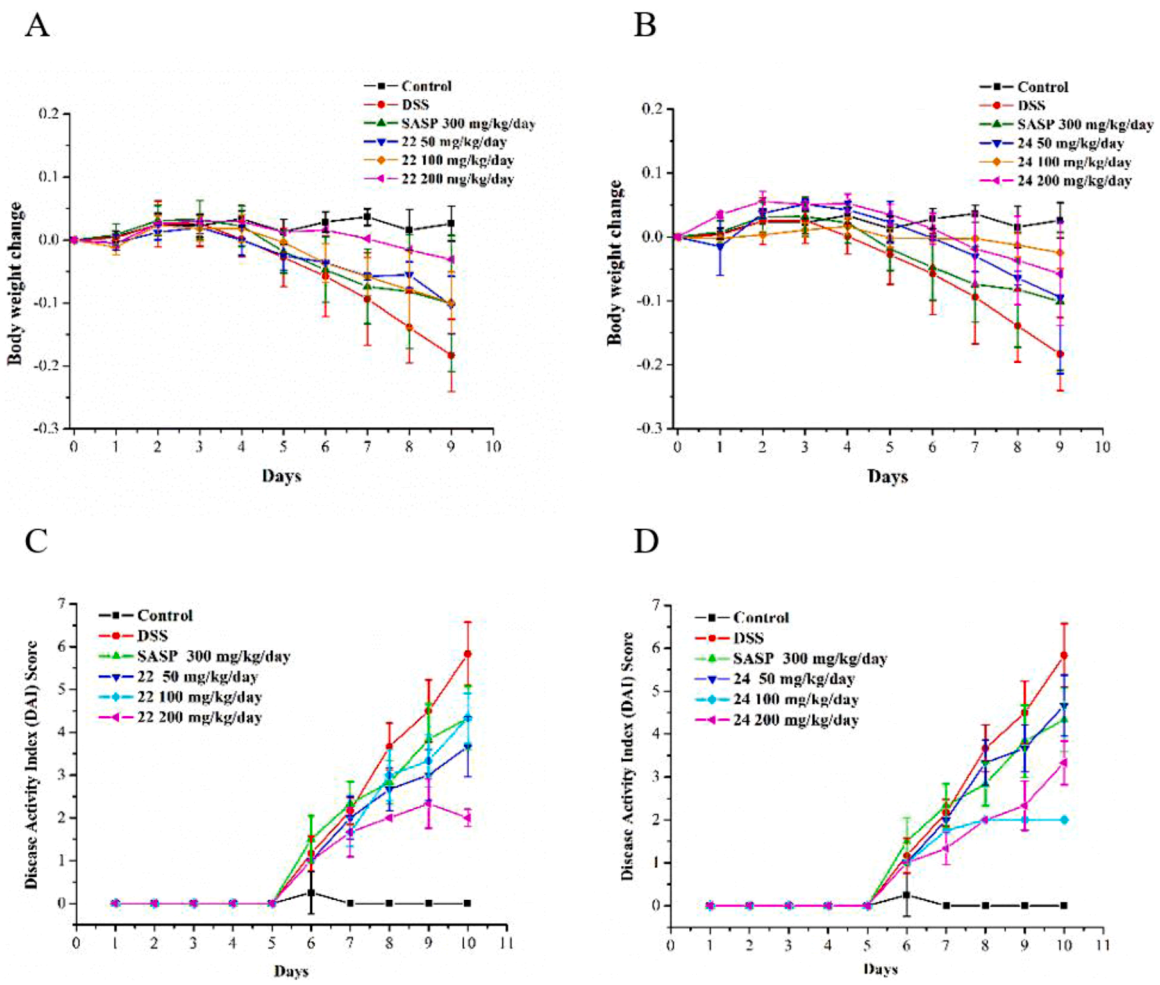

Fig. 10. Anti-inflammatory effects of **22** and **24** in DSS-induced colitis. (A and B) Body weight change. (C and D) DAI score. Data were expressed as means ± SD (n = 6).

Table 2
The DAI scoring system.

Score	Body weight loss (%)	Diarrhea	Rectal bleeding
0	0	normal	none
1	1–5		
2	6–10	loose stools	slight
3	10–15		
4	>15	diarrhea	fecal blood

Aldrich, Aladdin, Tan sole, Energy Chemical et al., without further purification.

4.1.1. *The synthesis of ortho-substituted mono-carbonyl curcumin derivatives*

The *ortho*-substituted mono-carbonyl curcumin derivatives together with acetone, cyclopentanone, cyclohexanone, or 4-piperidione (*N*—H or *N*-methyl) moieties were synthesized from *ortho*-substitued benzadehyde (2 equiv) and ketone (1.0 equiv) in ethanol (3 mol/L); and *ortho*-substituted *N*-acryloyl-4-piperidione-containing mono-carbonyl curcumin derivatives were synthesized from corresponding 4-piperidione-containing mono-carbonyl curcumin derivatives (1.0 equiv) and acryloyl chloride (1.5 equiv) in acetone (0.3 mol/L), according to our previously published paper. Their ^{1}H and ^{13}C nuclear magnetic (NMR) spectroscopy witnesses our previously published work (Liu et al., 2018; Liu and Zhang et al., 2018; Yang et al., 2018; Yang et al., 2018; Zhang et al., 2018).

4.2. *Cell lines and culture conditions*

The Raw264.7 cell line, which were obtained from the Shanghai Institute of Biochemistry and Cell Biology, Chinese Academy of Sciences, were cultured in DMEM (Hyclone) supplemented with 10% fetal bovine serum (Gibco), and 100 U/mL penicillin/streptomycin (Beyotime) in a humidified 5% CO_2 atmosphere at 37 °C (Thermo Scientific HERAceu150i).

4.3. *Measurement of the LPS-induced no production (Lee et al., 2009)*

100 μL Raw264.7 cells were seeded at 1 × 10^6 cells/well in 96-well plates (Costar) for 24 h and then incubated with LPS (Sigma) (1 μg/mL) and different concentrations of the test compounds for 24 h. Then 75 μL cell supernatant were mixed with the equal volumes of the fresh Griess reaction solutions (1% sulfanilamide, 0.1% *N*-(1-naphthyl)-ethylenediamine dihydro-chloride in 2.5% phosphoric acid) in a 96-well plate. After 5 min of incubation at RT, the absorbance at 540 nm was measured on a multiwallplate reader (Biotek Synergy H1 multi format microplate readers). Assays were performed in triplicate and repeated three times.

4.4. *Cell cytotoxic assay. (for 2.2.1)*

100 μL Raw264.7 cells were seeded at 1 × 10^6 cells/well in 96-well plates for 24 h and then treated with different concentrations of the test compounds for 24 h. After added the fresh solution of MTT (Beyotime) (10 μL, 5 mg/mL), the plate was incubated for an additional 4 h at 37 °C.

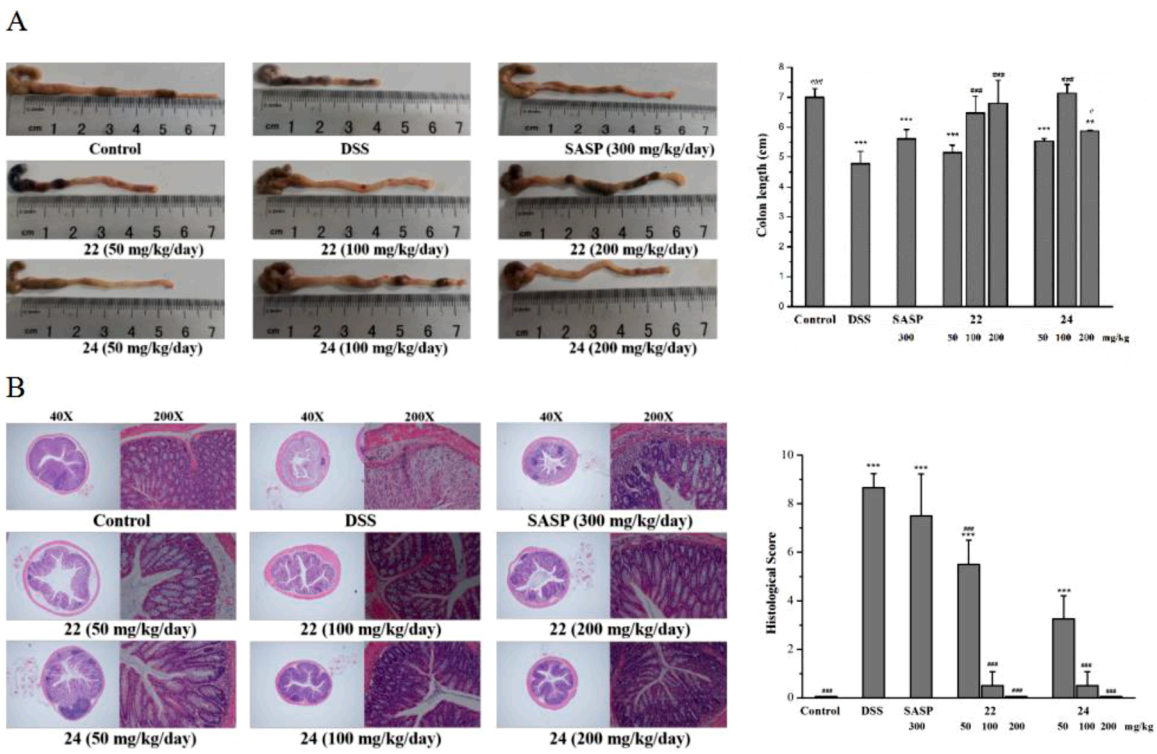

Fig. 11. Anti-inflammatory effects of **22** and **24** in DSS-induced colitis. (A) The length of colons. (B) The representative DSS-induced colonic pathological damage images (40x and 200x) and the histological scores. Data were expressed as means ± SD ($n = 6$). $^{*}p < 0.05$, $^{**}p < 0.01$, $^{***}p < 0.001$, compared with the control group; $^{\#}p < 0.05$, $^{\#\#}p < 0.01$, $^{\#\#\#}p < 0.001$, compared with the DSS-treated group. (For interpretation of the references to colour in this figure legend, the reader is referred to the web version of this article.)

Table 3
The histological scoring system.

Score	Severity of inflammation	Extent of inflammation	Crypt damage
0	none	none	none
1	mild	mucosa	1/3damaged
2	moderate	mucosa and submucosa	2/3damaged
3	severe	transmural	crypt loss by surface epithelium present
4			both crypt and surface epithelium lost

Finally, 300 μL of DMSO was added, and then 100 μL solution were distributed in a 96-well plate. The absorbance was measured at 570 nm by a multiwallplate reader (Biotek Synergy H1 multi format microplate readers). Assays were performed in triplicate and repeated three times.

4.5. *t*-BHP-induced oxidative cytotoxicity (for 2.2.2)

RAW 264.7 cells were grown in 96-well plates (2×10^4 cells/well, 100 μL/well) for 24 h, and then treated with different concentrations of compounds for 24 h. Cells were subsequently stimulated with *t*-BHP (2 mM) for an additional 3 h, and then washed with PBS buffer (10 mM, pH 7.4). MTT (100 μL, 0.5 mg/mL) was added to the cells and incubated for another 4 h. Then the supernatant was removed, and 150 μL DMSO was

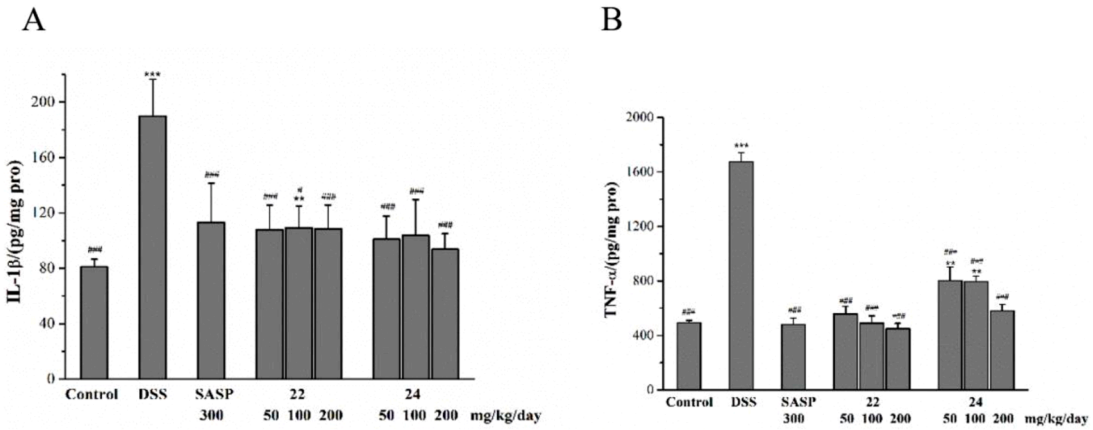

Fig. 12. Effects of the active compounds **22** and **24** on the production of IL-1β and TNF-α in DSS-induced colitis mice. (A) IL-1β levels. (B) TNF-α levels. Data were expressed as means ± SD ($n = 6$). $^{*}p < 0.05$, $^{**}p < 0.01$, $^{***}p < 0.001$, compared with the control group; $^{\#}p < 0.05$, $^{\#\#}p < 0.01$, $^{\#\#\#}p < 0.001$, compared with the DSS-treated group.

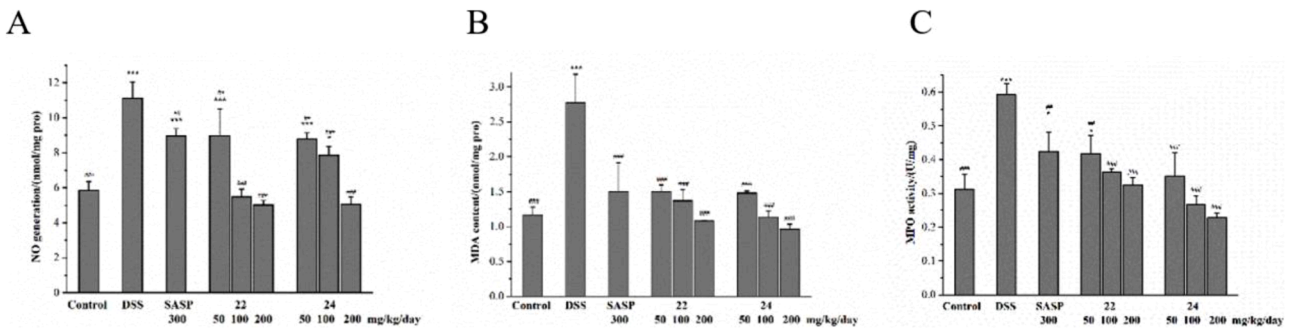

Fig. 13. Effects of **22** and **24** on NO production, MDA levels, and MPO activity in DSS-induced colitis mice. (A) NO production. (B) MDA levels. (C) MPO activity. Data were expressed as means ± SD ($n = 6$). $^{*}p < 0.05$, $^{**}p < 0.01$, $^{***}p < 0.001$, compared with the control group; $^{\#}p < 0.05$, $^{\#\#}p < 0.01$, $^{\#\#\#}p < 0.001$, compared with the DSS-treated group.

added to each well. The absorbance of MTT was measured at 570 nm by a microplate reader (Biotek Synergy H1 multi format microplate readers).

4.6. Cellular uptake activity

Raw264.7 cells were seeded at 3×10^6 cells/well (2 mL) in six-well plates and incubated for 24 h. After 0.5, 1, 2, 3, or 4 h of treatment with the test compounds **1, 10, 22** and **24** (50 μM), the cells were rapidly washed twice with 1 mL ice-cold PBS. They were then extracted with ice-cold methanol (800 μL/well) at 4 °C overnight. The suspension was centrifuged for 5 min at 10,000 rpm and 4 °C, and the supernatant (200 μL) was determined with high performance liquid chromatography (HPLC, Agilent Technologies 1260 Infinity). (Fig. 14)

After the cells were treated with **22** or **24** (50 μM) for 3 h, the cells (six wells) were rapidly washed twice with 1 mL ice-cold PBS, and then harvested. The samples were treated with the solution A of the membrane and cytosol protein extraction kit (Beyotime Biotechnology, China) to isolate cell membrane. Cell membrane was extracted with methanol (200 μL), and then the supernatant (200 μL) were determined with HPLC.

The standard curves were determined using 10 μL of 30, 20, 10 and 5 μM different compounds **1, 10, 22** and **24** in methanol solution. The methanol-water (90: 10) was used as mobile phase at the flow rate 1 mL/min. (**1**, 3.302 min, 373 nm, S (mAU*S) = 0.01093 + 12.3076 C (μM); **10**, 4.868 min, 350 nm, S (mAU*S) = −0.69604 + 10.07493 C (μM); **22**, 4.423 min, 310 nm, S (mAU*S) = 0.45776 + 14.72851 C (μM); **24**, 4.088 min, 310 nm, S (mAU*S) = 0.55896 + 16.22655 C (μM))

4.7. Determination of intracellular ROS levels (Yang et al., 2020)

Raw264.7 cells were seeded at 3×10^6 cells/well in six-well plates and incubated for 24 h. After treatment with LPS (1 μg/mL) and the test compounds for 24 h, the cells were collected, and washed twice with phosphate buffer solution (PBS, 10 mM, pH 7.4). And then resuspended in PBS and incubated with 3 μM DCFH-DA for 30 min at 37 °C in the dark. Then the cells were washed with PBS and analyzed immediately for DCFH-DA fluorescence intensity with a FACSCanto flow cytometer (Millipore Guava easyCyte 8HT benchtop flow cytometer) with excitation and emission settings of 488 and 530 nm, respectively. The 10,000 events were acquired per sample. Three independent experiments are carried out.

4.8. Cytokine assays

Raw264.7 cells were seeded at 3×10^6 cells/well in six-well plates for 24 h, and then treated with LPS (1 μg/mL) and different concentrations of the test compounds for 24 h. After incubation, the levels of IL-1β and TNF-α in the supernatant were measured using a mouse IL-1 beta ELISA Kit and a mouse TNF-alpha ELISA Kit (RayBiotech), following the manufacture's instructions.

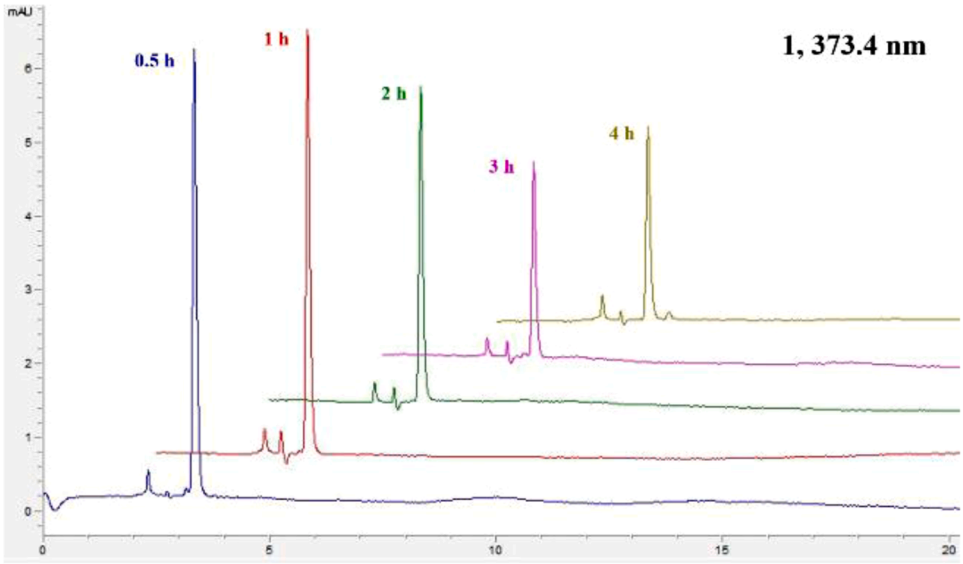

Fig. 14. The representative HPLC chromatogram of cellular uptake of **1** with different times.

4.9. Western blot analysis

Raw264.7 cells were seeded at 3×10^6 cells/well in six-well plates and incubated for 24 h. After treatment with LPS (1 μg/mL) and the test compounds for 24 h, the cells were harvested, washed twice with PBS, and lysed with radio immunoprecipitation Assay (RIPA) buffer (Beyotime) or nuclear extraction kits (Beyotime). And then western blot was carried out as the general process.

4.10. Animal

Balb/c mice (8-week-old, male, 18–20 g) were purchased from Pengyue Experimental Animal Breeding Co. LTD (Jinan, Shandong, China). Mice were housed on a 12 h dark/light cycle at constant temperature of 23 ± 2 °C with free access to standard diet and water. All animal studies were conducted under the National Institute Guide for the Care and Use of Laboratory Animals. Experimental protocols were approved by the Ethics Committee of Liaocheng University.

4.11. Induction of acute colitis and treatment

After 7 days of adaptation period, the animals were randomly assigned into nine groups ($n = 8$). Mice were supplied with distilled water ad libitum in the control group, whereas all other experimental groups were given 3.0% (w/v) DSS for 10 days. Besides, the mice of the SASP (300 mg/kg/day), **22** (50, 100, and 200 mg/kg/day), and **24** (50, 100, and 200 mg/kg/day) treated groups were orally given SASP, **22**, or **24** suspension with water from day 6 to day 10, respectively. Following the last administration, the mice were deprived food for 12 h, anesthetized, and sacrificed. Unfortunately, two mice of DSS-treated group dead in the experiment.

4.12. NO assay of colon tissues

The frozen colons were homogenized with 5 times volume PBS (10 mM, pH 7.4) containing proteinase inhibitors (Beyotime). The supernatants were obtained following centrifugation at 15,000 g at 4 °C for 20 min. The protein concentration of the supernatant was measured using Enhanced BCA Protein Assay Kit (Beyotime). The nitrite content in the supernatant was measured using the Griess reagent. The concentration of NO was calculated by extrapolating a $NaNO_2$ standard curve. The amounts of NO were expressed as nmol/mg tissue protein (nmol/mg).

4.13. MPO assay

40 μL of the supernatant of colons were added 60 μL PBS (50 mM, pH 6.0), 0.0005% *o*-dianisidine dihydrochloride, and 0.1% hydrogen peroxide. The rate of absorbance changes at 460 nm was measured. One unit of MPO activity is equal to 5.65×10^{-3} changes in absorbance at 25 °C. The activity of MPO was expressed as units/mg tissue protein (U/mg).

4.14. MDA assay

The amounts of MDA in the supernatants were determined using the Lipid Peroxidation MDA Assay Kit (Beyotime) as the manufactuer's instructions. The content of MDA was expressed as nmol MDA/mg tissue protein (nmol/mg).

4.15. Cytolines determination

The levels of IL-1β and TNF-α in the supernatants were determined using the Mouse IL-1β ELISA kit (ELM-1L1b-CL (for lysates), RayBiotech) and Mouse THF-α ELISA kit (ELM-TNFa-CL (for lysates), RayBiotech), according to the manufactuer's instructions.

4.16. Histopathology analysis

The colons of mice were fixed in buffered formalin (Beyotime), embedded in paraffin, and then sectioned. The sections were staining with hematoxylin and eosin (H&E), and photographed using an Olympus microscope (BX53 + DP80).

4.17. Statistical analysis

The data were presented as the means ± standard deviation (SD) and analyzed using one-way ANOVA to determine any significant differences. $p < 0.05$ was considered as statistically significant.

Declaration of Competing Interest

The authors declare no competing financial interest.

Acknowledgements

This work was supported by the National Natural Science Foundation of China (Grant No. 81901420).

References

Akira, S., Uematsu, S., Takeuchi, O., 2006. Pathogen recognition and innate immunity. Cell 124, 783–801.
Begum, A.N., Jones, M.R., Lim, G.P., Morihara, T., Kim, P., Heath, D.D., Rock, C.L., Pruitt, M.A., Yang, F.S., Hudspeth, B., Hu, S.X., Faull, K.F., Teter, B., Cole, G.M., Frautschy, S.A., 2008. Curcumin structure–function, bioavailability, and efficacy in models of neuroinflammation and alzheimer's disease. J. Pharmacol. Exp. Ther. 326, 196–208.
Bryant, R.V., Brain, O., Travis, S.P., 2015. Conventional drug therapy for inflammatory bowel disease. Scand. J. Gastroenterol. 50, 90–112.
Chawla, A., Nguyen, K.D., Goh, Y.P., 2011. Macrophage-mediated inflammation in metabolic disease. Nat. Rev. Immunol. 11, 738–749.
Chen, L.P., Li, Q., Weng, B.X., Wang, J.B., Wu, J.Z., 2018. Design, synthesis, anti-lung cancer activity, and chemosensitization of tumor-selective MCACs based on ROS-mediated JNK pathway activation and NF-κB pathway inhibition. Eur. J. Med. Chem. 151, 508–519.
Chen, T.P., Zhu, G.Y., Meng, X.W., Zhang, X.X., 2020. Recent developments of small molecules with anti-inflammatory activities for the treatment of acute lung injury. Eur. J. Med. Chem. 207, 112660–223679.
Chew, E.H., Nagle, A.A., Zhang, Y., Scarmagnani, S., Palaniappan, P., Bradshaw, T.D., Holmgren, A., Westwell, A.D., 2010. Cinnamaldehydes inhibit thioredoxin reductase and induce Nrf2: potential candidates for cancer therapy and chemoprevention. Free Radical Bio. Med. 48, 98–111.
Cooper, H.S., Murthy, S.N., Shah, R.S., Sedergran, D.J., 1993. Clinicopathologic study of dextran sulfate sodium experimental murine colitis. Lab. Invest. 69, 238–249.
Cosnes, J., Gower-Rousseau, C., Seksik, P., Cortot, A., 2011. Epidemiology and natural history of inflammatory bowel diseases. Gastroenterology 140, 1785–1794.
Dai, F., Liu, G.Y., Li, Y., Yan, W.J., Wang, Q., Yang, J., Lu, D.L., Ding, D.J., Lin, D., Zhou, B., 2015. Insights into the importance for designing curcumin-inspired anticancer agents by a prooxidant strategy: the case of diarylpentanoids. Free Radical Bio. Med. 85, 127–137.
Dinkova-Kostova, A.T., Cory, A.H., Bozak, R.E., Hicks, R.J., Cory, J.G., 2007. Bis(2-hydroxybenzylidene)acetone, a potent inducer of the phase 2 response, causes apoptosis in mouse leukemia cells through a p53-independent, caspase-mediated pathway. Cancer Lett 245, 341–349.
Dinkova-Kostova, A.T., Massiah, M.A., Bozak, R.E., Hicks, R.J., Talalay, P., 2001. Potency of Michael reaction acceptors as inducers of enzymes that protect against carcinogenesis depends on their reactivity with sulfhydryl groups. Proc. Natl. Acad. Sci. USA 98, 3404–3409.
Dudzińska, E., Gryzinska, M., Ognik, K., Gil-Kulik, P., Kocki, J., 2018. Oxidative stress and effect of treatment on the oxidation product decomposition processes in IBD. Oxid. Med. Cell. Longev. Article ID 7918261, 7 pages.
Gan, F.F., Kaminska, K.K., Yang, H., Liew, C.Y., Leow, P.C., So, C.L., Tu, L.N., Roy, A., Yap, C.W., Kang, T.S., 2013. Identification of Michael acceptor-centric pharmacophores with substituents that yield strong thioredoxin reductase inhibitory character correlated to antiproliferative activity. Antioxid. Redox Signal. 19, 1149–1165.
Hagmann, W.K., 2008. The many roles for fluorine in medicinal chemistry. J. Med. Chem. 51, 4359–4369.
Harbord, M., Eliakim, R., Bettenworth, D., Karmiris, K., Katsanos, K., Kopylov, U., Kucharzik, T., Molnár, T., Raine, T., Sebastian, S., 2017. Third European evidence-based consensus on diagnosis and management of ulcerative colitis. Part 2: current management. J. Crohn's Colitis 11, 769–784.
He, Y., Li, W., Hu, G., Sun, H., Kong, Q., 2018. Bioactivities of EF24, a Novel Curcumin Analog: a Review. Front. Oncol. 8, 614–622.

Karimian, M.S., Pirro, M., Majeed, M., Sahebkar, A., 2017. Curcumin as a natural regulator of monocyte chemoattractant protein-1. Cytokine Growth F. R. 33, 55–63.
Kawalec, P., Malinowski, K.P., 2015. Indirect health costs in ulcerative colitis and Crohn's disease: a systematic review and meta-analysis. Expert Rev. Pharm. Outcomes Res. 15, 253–266.
Kim, Y.S., Ahn, C.B., Je, Y.J., 2016. Anti-inflammatory action of high molecular weight Mytilus edulis hydrolysates fraction in LPS-induced RAW264.7 macrophage via NF-kappaB and MAPK pathways. Food Chem. 202, 9–14.
Kunwar, A., Barik, A., Mishra, B., Rathinasamy, K., Pandey, R., Priyadarsini, K., 2008. Quantitative cellular uptake, localization and cytotoxicity of curcumin in normal and tumor cells. Biochi. Biophys. Acta 1780, 673–679.
Lee, Y.G., Chain, B.M., Cho, J.Y., 2009. Distinct role of spleen tyrosine kinase in the early phosphorylation of inhibitor of kappaB alpha via activation of the phosphoinositide-3-kinase and Akt pathways. Int. J. Biochem. Cell Biol. 41, 811–821.
Lei, Y., Wang, K., Deng, L., Chen, Y., Nice, E.C., Huang, C., 2015. Redox regulation of inflammation: old elements, a new story. Med. Res. Rev. 35, 306–340.
Li, W., He, Y.H., Zhang, R.P., Zheng, G.R., Zhou, D.H., 2019. The curcumin analog EF24 is a novel senolytic agent. Aging 11, 771–782.
Liu, G.Y., Jia, C.C., Han, P.R., Yang, J., 2018a. 3,5-Bis(2-fluorobenzylidene)-4-piperidone induce reactive oxygen species-mediated apoptosis in A549 cells. Med. Chem. Res. 27, 128–136.
Liu, G.Y., Zhai, Q., Chen, J.Z., Zhang, Z.Q., Yang, J., 2016. 2,2′-Fluorine mono-carbonyl curcumin induce reactive oxygen species-Mediated apoptosis in Human lung cancer NCI-H460 cells. Eur. J. Pharmacol. 786, 161–168.
Liu, G.Y., Zhang, Q., Xue, Y.X., Zhang, H.L., Yang, J., 2018b. Piperidone substituted curcumin analogs exert potent anticancer activity by inducing apoptosis. Chin. J. Syn. Chem. 26, 354–359.
Liu, Z.F., Li, Z.J., Du, T., Chen, Y., Wang, Q.P., Li, G.S., Liu, M., Zhang, N., Li, D.C., Han, J., 2021. Design, synthesis and biological evaluation of dihydro-2-quinolone platinus (IV) hybrids as antitumor agents displaying mitochondria injury and DNA damage mechanism. Dalton Trans 50, 362–375.
Mazzucchelli, L., Hauser, C., Zgraggen, K., Wagner, H., Hess, M., Laissue, J.A., Mueller, C., 1994. Expression of interleukin-8 gene in inflammatory bowel disease is related to the histological grade of active inflammation. Am. J. Pathol. 144, 997–1007.
Mittal, M., Siddiqui, M.R., Tran, K., Reddy, S.P., Malik, A.B., 2014. Reactive oxygen species in inflammation and tissue injury. Antioxid. Redox. Sign. 20, 1126–1167.
Mu, H.X., Liu, J., Fatima, S., Lin, C.Y., Shi, X.K., Du, B., Xiao, H.T., Fan, B.M., Bian, Z.X., 2016. Anti-inflammatory actions of (+)-3'α-angeloxy-4'-keto-3',4'-dihydroseselin (Pd-Ib) against dextran sulfate sodium-induced colitis in C57BL/6 mice. J. Nat. Prod. 79, 1056–1062.
Müller, K., Faeh, L., Diederich, F., 2007. Fluorine in Pharmaceuticals: looking Beyond Intuition. Science 17, 1881–1886.
Nagy, G., Clark, J.M., Buzas, E.I., Gorman, C.I., Cope, A.P., 2007. Nitric oxide, charonic inflammation and autoimmunity. Immunol. Lett. 111, 1–5.
Schönherr, H., Cernak, T., 2013. Profound methyl effects in drug discovery and a call for new C-H methylation reactions. Angew. Chem. Int. Ed. 52, 12256–12267.
Singh, A., Singh, J.V., Rana, A., Bhagat, K., Gulati, H.V., Kumar, R., Salwan, R., Bhagat, K., Kaur, G., Singh, N., Kumar, R., Singh, H., Sharma, S., Singh Bedi, P.M., 2019. Monocarbonyl curcumin-based molecular hybrids as potent antibacterial agents. ACS Omega 4, 11673–11684.
Singh, K., Jaggi, A.S., Singh, N., 2009. Exploring the ameliorative potential of punica granatum in dextran sulfate sodium induced ulcerative colitis in mice. Phytother. Res. 23, 1565–1574.
Siviero, A., Gallo, E., Maggini, V., Gori, L.G., Mugelli, A., Firenzuoli, F., Vannacci, A., 2015. Curcumin, a golden spice with a low bioavailability. J. Herb. Med. 5, 57–70.
Wiggers, H.J., Zaioncz, S., Cheleski, J., Mainardes, R.M., Khalil, N.M., 2017. Chapter 7-Curcumin, a multitarget phytochemical: challenges and perspectives. Stud. Nat. Prod. Chem. 53, 243–276.
Wu, J.Z., Zhang, Y.L., Cai, Y.P., Wang, J.B., Weng, X., Tang, Q.Q., Chen, X.J., Pan, Z., Liang, G., Yang, S.L., 2013. Discovery and evaluation of piperid-4-one-containing mono-carbonyl analogs of curcumin as anti-inflammatory agents. Bioorganic Med. Chem. 21, 3058–3065.
Yang, J., Mu, W.W., Cao, Y.X., Liu, G.Y., 2020. Synthesis and biological evaluation of β-ionone oriented proapoptosis agents by enhancing the ROS generation. Bioorg. Chem. 104, 104273.
Yang, J., Shi, Y.M., Li, G.Y., Huang, Y.Y., Zhang, Y., Zhang, H.L., Liu, G.Y., 2018a. In vitro antitumor activity of newly synthesized EF24 analog via apoptosis induction. Lat. Am. J. Pharm. 37, 2033–2039.
Yang, J., Zhao, Y.J., Li, X.J., Meng, S.S., Zhang, H.L., Liu, G.G., 2018b. Synthesis of trifluoromethyl-substituted mono-carbonyl curcumin analogs and evaluation of their anti-proliferation activity on lung cancer cells. J. Int. Pharm. Res. 45, 593–596.
Yerien, D.E., Bonesi, S., Postigo, A., 2016. Fluorination methods in drug discovery. Org. Biomol. Chem. 14, 8398–8427.
Yu, J., Yao, H., Gao, X., Zhang, Z., Wang, J.F., Xu, S.W., 2015. The role of nitric oxide and oxidative stress in intestinal damage induced by selenium deficiency in chickens. Biol. Trace Elem. Res. 163, 144–153.
Zhang, H.L., Ren, X.L., Yang, W.H., Xie, Y., Yang, J., Liu, G.Y., Guo, S.J., 2018. Synthesis and evaluation of anti-cancer activities of mono-carbonyl curcumin analogs. Lat. Am. J. Pharm. 37, 958–963.
Zhou, Y., Zhang, T., Wang, X., Wei, X., Chen, Y., Guo, L., Zhang, J., Wang, C., 2015. Curcumin modulates macrophage polarization through the inhibition of the toll-like receptor 4 expression and its signaling pathways. Cellular Physiol. Biochem. 36, 631–641.
Zhu, H.P., Xu, T.T., Qiu, C.Y., Wu, B.B., Zhang, Y.L., Chen, L.F., Xia, Q.Q., Li, C.L., Zhou, B., Liu, Z.G., Liang, G., 2016. Synthesis and optimization of novel allylated mono-carbonyl analogs of curcumin (MACs) act as potent anti-inflammatory agents against LPS-induced acute lung injury (ALI) in rats. Eur. J. Med. Chem. 121, 181–193.